



## Accepted Manuscript

**Geochemical characteristics and paleogeographic analysis of the Late Cretaceous (Ilam Formation) in the Lorestan subzone, Zagros area, Iran**

**Atefeh Yeganeh Moghadam, Asadollah Mahboubi, Mohammad Hosein Mahmoudi Gharaei, Reza Moussavi Harami**

DOI: 10.22059/GEOPE.2025.389942.648804

Receive Date: 04 February 2025

Revise Date: 18 February 2025

Accept Date: 03 March 2025

## Geochemical characteristics and paleogeographic analysis of the Late Cretaceous (Ilam Formation) in the Lorestan subzone, Zagros area, Iran

Atefeh Yeganeh Moghadam, Asadollah Mahboubi \*, Mohammad Hosein Mahmoudi Gharaei, Reza Moussavi Harami

Department of Geology, Faculty of Science, Ferdowsi University of Mashhad, Mashhad, Iran

Received: 04 February 2025, Revised: 18 February 2025, Accepted: 03 March 2025

© University of Tehran

### Abstract

The Ilam Formation in the Zagros basin, southwest Iran, is a rich petroleum reservoir rock that possesses considerable exploration potential. This study provides valuable insights into the paleoenvironmental and paleogeographic conditions of the Ilam Formation using sedimentological and geochemical analysis as well as sea-level changes during the Late Cretaceous time (Late Santonian-Late Campanian) in the Lorestan area. Based on petrographic analysis, four microfacies were identified in the studied area (Mehdi Abad section) in the Ilam Formation that were deposited in an outer ramp setting, from middle neritic to bathyal, in a homoclinal ramp. Sequence stratigraphic analysis led to detect two transgressive system tracts and one regressive system tract. In the current study, the paleo-geochemical signatures, using redox-sensitive elements, show strong evidence of declining oxygen level during the Late Santonian and Late Campanian; however, increase of oxygen levels only observed during the Early Campanian time. The changes in oxic-anoxic conditions in the depositional basin during deposition of the Ilam Formation can be correlated with the final phase of the oceanic anoxic event in the Cretaceous. However, the closure event of the Neo-Tethys Ocean and subsequent changes in fault mechanisms and basin structure were causal mechanisms of oxic-anoxic conditions during this period.

**Keywords:** Ilam Formation, Late Santonian- Late Campanian, Oxic-Anoxic Conditions, Neo-Tethys Ocean, Redox-Sensitive Elements.

### Introduction

The southwestern region of Iran is recognized as a highly productive area for oil and gas, boasting substantial proven reserves. These reservoirs are mostly developed in the Permo-Triassic, Cretaceous, and Oligo-Miocene intervals of the Zagros basin (Motiei, 1995). The Late Cretaceous time in the Zagros area of Iran is characterized by the occurrence of several large-scale events including significant tectonic episodes, global sea-level changes, and an increase in greenhouse gases and trends in temperature (e.g., Berberian and King, 1981; Agard et al., 2005; Kordi, 2019; Razmjooei et al., 2020). These events led to the vast development of petroliferous rock units and carbonate hydrocarbon reservoirs in this area (Pitman et al., 2004; Liu et al., 2018).

The Bangestan Group, with the Albian to Campanian age, including Kazhdomi, Sarvak, Surgah, and Ilam Formations is considered the second most important oil reservoir of Iran after the Oligo-Miocene Asmari Formation, with approximately 37% of Iran's proven petroleum in-place (Motiei, 1993). The Upper Cretaceous carbonate rocks of the Ilam Formation represent

---

\* Corresponding author e-mail: Mahboubi@um.ac.ir

remarkable reservoirs producing hydrocarbon in the Dezful Embayment and Lorestan subzones of the Zagros Basin. The Ilam Formation is largely composed of argillaceous limestone, marl, and limestone layers in the Lorestan subzone.

Most studies carried out on the Ilam Formation have focused on biostratigraphy aspects and duration of sedimentation (Motiei, 1993; Rikhtehgarzadeh et al., 2017; Shafiee Ardestani et al., 2022; Abasaghi and Omidpour, 2023), or on reservoir zonation and petrophysical analysis (Kosari et al., 2017; Mehrabi et al., 2022; Ounegh et al., 2024), especially in the Dezful Embayment. In spite of the successful outcomes of these studies, more studies are still needed to reveal the geochemical characteristics of the Ilam Formation in relation to depositional settings and paleogeographic conditions. Indeed, until now, there has been a notable deficiency in a comprehensive examination of detailed chemical elements in the intervals of the Ilam Formation, particularly in the Lorestan subzone.

The utilization of certain elements as paleoenvironmental analysis has grown significantly over the past decades. It is proven that some trace and Rare-Earth Elements, called redox-sensitive elements (RSEs), can be considered as quantitative means and paleo-redox indicators that can be used to interpret the transition from oxic to anoxic conditions, as their distribution is governed by environmental parameters and climatic conditions. Additionally, they are also widely used in interpreting sediment sources, tectonic settings, and even stratigraphic correlation (e.g., Van Cappellen & Ingall, 1996; Tribovillard et al., 2006; Yang et al., 2012; Jones et al., 2018; Kouamelan et al., 2020; Zheng et al., 2024).

One of the most significant geologic events of the Cretaceous period, as categorized in paleo-redox studies, is the Oceanic Anoxic Event (OAE). This event has long received extensive attention from researchers. OAEs are defined by episodes of organic accumulation, an increase in atmospheric CO<sub>2</sub>, enrichment or depletion of RSEs, changes in carbon isotope excursion, severe oxygen exhaustion, an enhanced greenhouse effect, and global warming (e.g., Arthur et al., 1990; Beckman et al., 2005; Tejada et al., 2009; Sachse et al., 2012; Jones et al., 2018; Kouamelan et al., 2020; Jafarian et al., 2024). Evidence of this event has also been identified in the Cretaceous intervals of the Zagros area (Jafarian et al., 2024).

In the current study, the Ilam Formation in the Lorestan subzone was chosen for examination of the geochemical characteristics during the Late Cretaceous time. The Cretaceous strata in the Lorestan subzone in the west of Iran include the Garu, Sarvak, Surgah, Ilam, and Gurpi Formations, which consist of carbonate, marl, and organic-rich shale lithologies. The deposition of these successions has been controlled by the tectonic phases of the Zagros orogeny and is mostly related to passive margin settings. The objectives of this study are as follows: 1) to identify sedimentary facies and establish a depositional model for the Ilam Formation during the Santonian-Campanian, 2) to analyze the geochemical features of the carbonate strata within the Ilam Formation, and 3) to explain paleogeographic control on the evolution of basin during the Late Cretaceous time in the Lorestan subzone of the Zagros.

## **Geological background**

The Lorestan subzone located in the west of Iran is one of the tectono-sedimentary units of the Zagros fold-thrust belt (Alavi, 1994; McQuarrie, 2004). Considering the sedimentary and structural history, the Zagros fold-thrust belt is divided into tectono-stratigraphic domains of Izeh, Lorestan, Dezful Embayment, Fars, and High Zagros (Figure 1a) (Falcon, 1974; Sherkati and Letouzey, 2004). The NW-SE trending of the Zagros orogenic belt is inherited from the closure event of the Neo-Tethys Ocean during the Late Cretaceous to the Neogene time. In fact, the Zagros range is a collisional belt between the Arabian Plate and the Iranian Block and its zones trend parallel to the plate suture (Berberian and King, 1981).

The evolution of the Zagros fold-thrust belt, along with its corresponding foreland basin from

the Mesozoic to Cenozoic, can be categorized into two distinct phases. The first phase, lasting from the Triassic to the Turonian, saw the Zagros located on the northeastern passive margin of the Arabian plate. The second phase extending from the Turonian to the present, is attributed to the transition of the northeastern Arabian plate into an active continental margin (Agard et al., 2005; Karimnejad Lalami et al., 2020).

The Ilam Formation in the Zagros area deposited during the Santonian to the Campanian time (James and Wynd, 1965). The formations of Fiqa, Aruma, Ghadir, Kometan-Shiranish, and Halul in the Arabian Plate are time-equivalent intervals of Ilam Formation (Alsharhan and Nairn, 1997).

The Lorestan subzone contains 10-14 km stratigraphic successions from the Paleozoic to Cenozoic, stretching approximately 300 km long and up to 200 km wide. In the Lorestan subzone, the Ilam Formation has been deposited unconformably above the black shale layers of the Surgah Formation and is overlapped disconformably by pelagic carbonates and shale layers of the Gurpi Formation (Figures 2a and 2b). However, in some areas, it is difficult to separate and define their boundaries with each other due to similar lithologies.

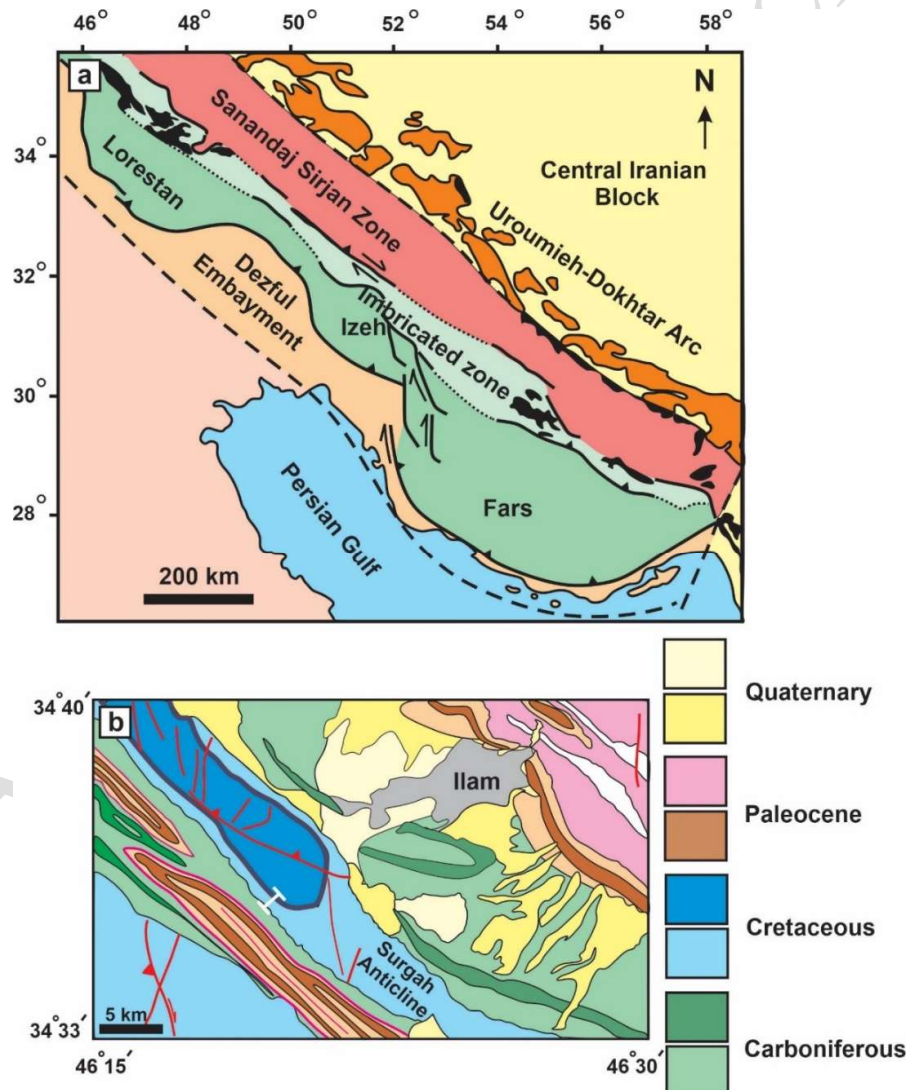


**Figure 1.** a) Subdivision of the Zagros fold-thrust belt including the studied area (after Alavi, 1994) b) A part of 1/100000 Ilam geological map (after Sedaghat and Shaverdi, 1999). The geographic coordinates of the Mehdi-Abad section are N 46° 19' and E 34° 35'

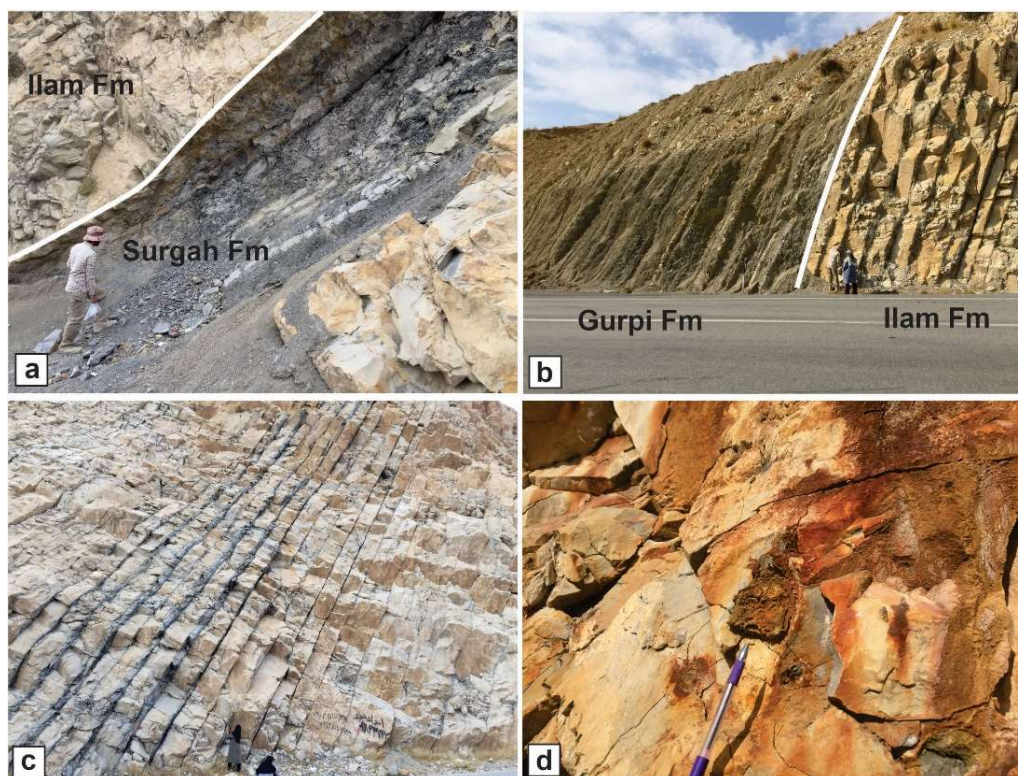


**Figure 2.** a) The boundary between the Surgah and Ilam Formations, b) The boundary between the Ilam and Gurpi Formations, c) Gray limestone layers with interbedded shale layers of the Ilam Formation, d) The hematite nodules at lower intervals of the Ilam Formation

The Upper Cretaceous Ilam Formation is composed of light and dark gray limestone, with interbedded black shales (Figure 2c). Hematite nodules are observed in the lower intervals of the Ilam Formation in the Mehdi-Abad section (Figure 2d). The Mehdi-Abad section, located southwest of Ilam town in the Lorestan subzone in the Surgah anticline and was chosen for the current study (Figure 1b), because this is the only place that can be seen the top and base of the Ilam Formation in the study area. The Ilam Formation in the Mehdi-Abad section consists of 193 meters of brown to gray limestone, argillaceous limestone, and black shales (Figure 3). A planktonic foraminiferal biozonation consisting of five biozones (1- *Dicarinella asymetrica*, 2- *Globo truncanita elevate*, 3- *Globo truncana ventricosa*, 4- *Radotruncana calcarata*, 5- *Globo truncanella havanesis*, and 6- *Globo truncana aegyptiaca*) is proposed for dating the Ilam Formation in the Mehdi-Abad section. The identified biozones suggest a Late Santonian-Late Campanian (Late Cretaceous) age for the Ilam Formation at this location (Bohlouli, 2020).

### Materials and methods

During fieldwork and the process of systematic sampling from the Mehdi-Abad section, a total of 130 rock samples were collected for petrographic and geochemical analyses. Thin sections were prepared for petrographical studies. The classification scheme of Dunham (1962) was used to describe carbonate rocks of the Ilam Formation. We compared our identified microfacies with standard models of Read (1985) and Flügel (2010) to interpret depositional environment of the Ilam Formation in the study area. Identification of system tracts and sequence stratigraphy analysis was performed using the Hunt and Tucker (1992) and Catnueanu et al. (2011) models

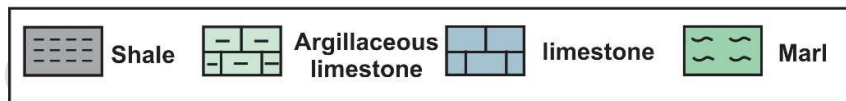
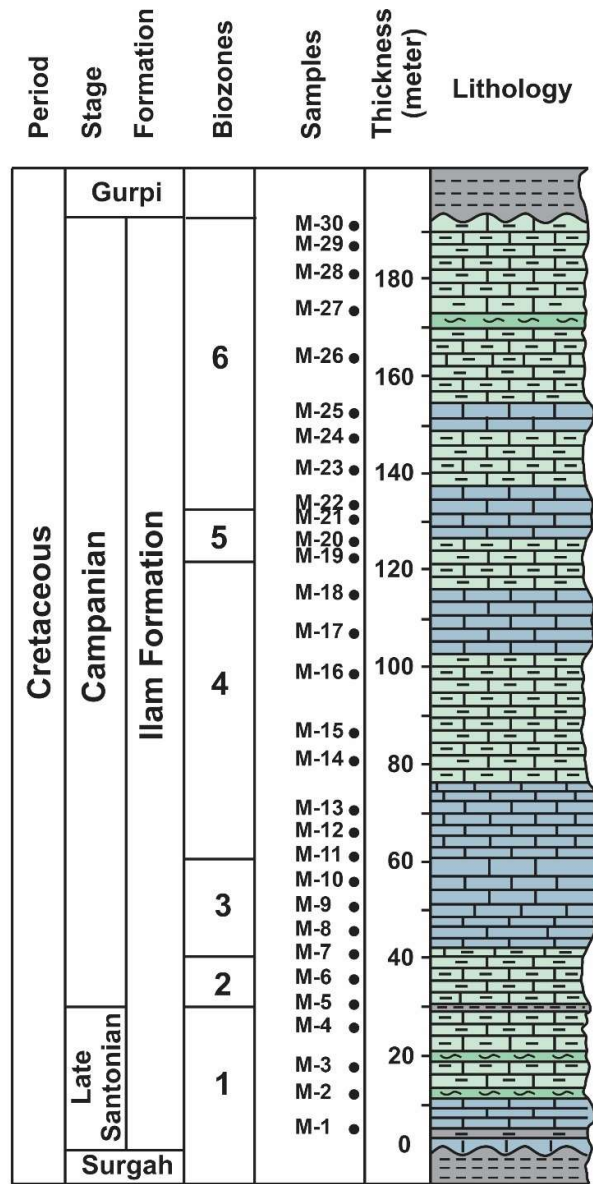


**Figure 3.** The stratigraphic column of the Ilam Formation in the Mehdi-Abad section, associated with position of collected samples (M-1 to M-30) for geochemical analysis. The range of identified biozones by Bohlouli (2020) are shown on the column

For conducting geochemical analysis and determination of certain elements using method of Inductively Coupled Plasma Mass Spectroscopy (ICP-MS), 5 grams powder from 30 carbonate samples were sent to Zar Azma laboratory in Tehran, Iran. The stratigraphic positions of these samples are shown in Figure 3. The chosen samples were from those samples that had muddy texture without diagenesis imprints and remnants of skeletal debris. ICP-MS is an analytical technique that works based on ionization of elements within each sample by applying electrical energy. In this process, 0.25 grams of powder from each sample were treated with HNO<sub>3</sub>, HClO<sub>4</sub>, HCl, and HF to dissolve of solid materials. The resulting solutions were subjected to hot argon plasma that led to emission of energy with specific wavelengths for each chemical element.

In order to determine the mineralogical composition of shale intervals in the Ilam Formation, 5 grams of four powder samples were analyzed using X-ray diffraction analysis (XRD) in the laboratory of the Geological Survey of Iran. In this method, organic matters, carbonate constitutes, and oxides were removed from samples. Various treatments were then applied, including heating to 550° Celsius, and saturation with magnesium chloride, ethylene glycol, and potassium chloride. In the final stage, X-ray spectra with specific wavelengths that were generated during the irradiation of prepared samples allowed for the identification of clay minerals.

## Results

### *Microfacies*

The petrographic analysis led to the identification of four microfacies including:

#### Mudstone to mudstone with planktonic foraminifera (MF1)

This microfacies is mostly found in thin beds of gray limestones and argillaceous limestones from the lower and upper parts of the outcrop, which are intercalated with black shale laminae. It contains small amounts of grains, approximately 5%, while the rest of the rock is relatively composed of dark micrite (Figure 4a). In some samples, planktonic foraminifera are present with less than 10% abundance. This microfacies is rich in organic matter and pyrite grains at places.

#### Wackestone with planktonic foraminifera (MF2)

At the outcrop, the intervals including MF2 are thin to medium-thick limestone interbedded with argillaceous limestone and shale. These intervals correspond to 16-50 meters at the base and 120-183 meters at the top of outcrop. In this microfacies, the relative abundance of planktonic foraminifera ranges from 30-45 % (Figure 4b). Most planktonic foraminifera consist of *Globotruncana*, *Dicarinella*, *Marginotruncana*, *Globotruncanella*, and a few *Pseudotextularia*. The significant presence of organic matter, accompanied by minor occurrence of pyrite and phosphate, is remarkable in this microfacies.

#### Wackestone-packstone with planktonic foraminifera and oligosteginids (MF3)

This microfacies is identified within medium to thick limestone intervals in the outcrop. The texture of this microfacies ranges from wackestone to packstone. MF3 exhibits most development between 40 and 150 meters in the outcrop. The total relative abundance of grains of this microfacies is 20 to 65 %. Most skeletal constituents include planktonic foraminifera and oligosteginids along with minor to moderate presence of organic matter (Figure 4c). The dominant genera of planktonic foraminifera in this microfacies are *Globotruncana*, *Macroglobigerinelloides*, *Archaeglobigerina*, *Heterohelix*, *Dicarinella*, *Marginotruncana*, *Rugoglobigerina*, *Globotruncanella*, and *Contusotruncana*.

#### Wackestone-packstone with planktonic foraminifera and skeletal fragments (MF4)

The thickness of limestone layers belonging to this microfacies is relatively more than other microfacies. They are associated with argillaceous limestones. The texture of this microfacies ranges from wackestone to packstone. MF4 has been deposited in the middle parts of the section, ranging from 50 to 115 meters. This microfacies comprises well-preserved planktonic foraminifera and skeletal fragments with a percentage of 30 to 70% (Figure 4d). Rare

oligosteginids are present in this microfacies. The identified planktonic foraminifera are similar to those in MF3. The present skeletal grains in this microfacies are small fragments of bivalve, bryozoan, sponge, and brachiopods. The organic matters and pyrite grains are also observed but with lower percentages compared to with previous microfacies.

### ***Geochemical analysis***

#### *Mineralogy*

In order to identify clay minerals present in shale samples from the Ilam Formation, four samples were analyzed using XRD. Based on XRD results, kaolinite is the most abundant mineral in the shale samples, however lower amounts of illite, and montmorillonite are also detected (Figure 5). The associated non-clay minerals include calcite, quartz, albite, and hematite.

#### ***Trace elements***

The results are presented in Table 1, the ICP-MS detected elements including vanadium (5 - 13.4 ppm), chromium (2-7.5 ppm), nickel (8-14 ppm), cobalt (1-3.4 ppm), thorium (0.2 - 1.2 ppm), uranium (0.2 - 6 ppm), molybdenum (1.4 - 58 ppm), iron (368- 1245 ppm), manganese (106-392 ppm), strontium (109 -1101 ppm), and sodium (105-301 ppm) in the carbonate samples of the Ilam Formation. As seen in Table 1, Fe, Mn, Sr, and Na exceed 100 ppm with a wide range, while the elements of V, Cr, Ni, Co, Th, U, and Mo show lower values and define a narrower range.

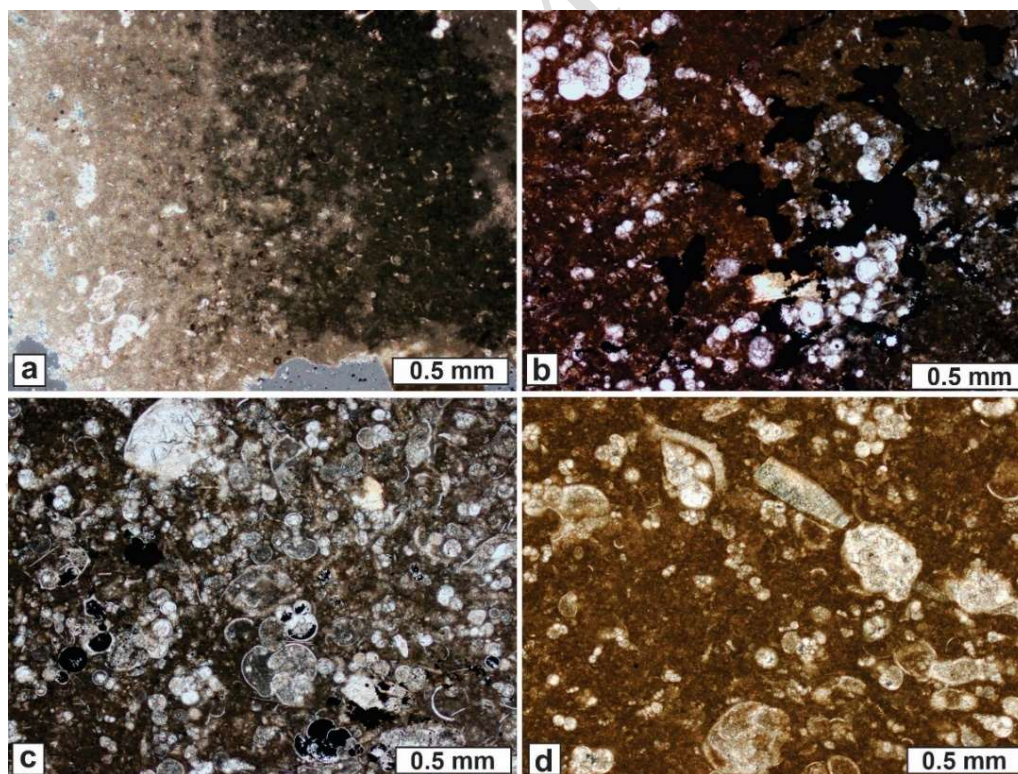


**Figure 4.** The identified microfacies of the Ilam Formation, a) Mudstone to mudstone with planktonic foraminifera (XPL), b) Wackestone with planktonic foraminifera (XPL), c) Wackestone-packstone with planktonic foraminifera and oligosteginids (XPL), d) Wackestone-packstone with planktonic foraminifera and skeletal fragments (XPL)

Numerous studies have proved that certain ratios of redox-sensitive elements are useful for further clarification about paleoredox conditions. In this study, the ratios of V/Cr, Ni/Co, V/V+Ni, Th/U, and V/Mo were used as good criteria to differentiate samples that were deposited in oxic conditions from those samples that were deposited under anoxic environments. The analytical results of these ratios have presented in Figure 6.

**Table 1.** Trace elements concentration (ppm) of the carbonate samples of the Ilam Formation, Mehdi-Abad section

	Co	Cr	Mo	Ni	Th	U	V	Sr	Na	Fe	Mn
M-1	1.2	2.3	25	9	0.4	5.3	47.2	430	175	947	325
M-2	1.4	2.8	32	10.1	1.2	6	65	762	105	957	357
M-3	1.3	2	7.1	9.5	0.6	2	39.7	542	124	832	392
M-4	1.4	3	34	10.8	0.3	4.5	53.4	398	120	1245	384
M-5	1.8	2.4	6.3	13.5	0.2	6	42	857	118	1204	303
M-6	2	3.5	2	12	0.5	1	13	964	256	436	106
M-7	1.5	3.7	3.9	9.4	0.6	0.2	12.2	1053	301	505	127
M-8	1.6	3.9	4	9.5	0.8	0.3	8.3	863	248	671	108
M-9	1.4	5.2	1.5	8.9	0.5	0.4	7	1101	230	658	302
M-10	3.1	4.5	1.4	9	0.7	0.3	5	836	261	642	169
M-11	3.4	4	1.5	9.1	0.8	2	6.2	839	255	640	201
M-12	2.5	4.1	4	8	0.4	1.8	15.8	740	242	443	253
M-13	2.1	3.2	2.5	10.3	0.7	3.5	5	759	203	904	264
M-14	2.3	4.5	3.4	13	0.4	2.1	18	352	173	590	297
M-15	2.6	3.1	3	12.8	1	5.1	6.6	531	185	623	204
M-16	3	3.5	1.8	12.5	0.8	0.7	5.7	438	210	429	142
M-17	3.1	3.4	3	13.2	0.6	1.5	5.9	389	174	368	198
M-18	2.2	4.7	6.9	12	0.9	1.8	17.1	370	183	388	106
M-19	2.8	6.4	20.5	14	0.4	0.7	38	368	265	573	207
M-20	2.6	7.5	5.6	13	0.6	1	30	403	149	705	185
M-21	1.5	4.3	4	12.8	0.7	1.4	17.6	360	237	1005	297
M-22	1.4	5.8	10	12	0.7	1	21.5	345	190	960	286
M-23	1.2	2.6	38.5	12.5	0.8	1.3	62	244	205	658	250
M-24	1	2.6	35.6	9	0.2	0.7	51.5	268	188	693	247
M-25	1.1	2.8	42	8	0.6	3.5	53	109	195	570	309
M-26	1.3	2.7	56	10.2	0.5	4.8	62.6	396	174	849	384
M-27	1.1	2.6	58	9	0.9	5	62.8	477	125	796	362
M-28	1.4	2.4	46	11.5	0.3	6	61.7	368	116	905	352
M-29	1.8	2.7	55	13	0.3	4.8	73	274	131	1105	367
M-30	1.6	2.5	40.3	11.6	0.4	4	48.1	305	109	758	359

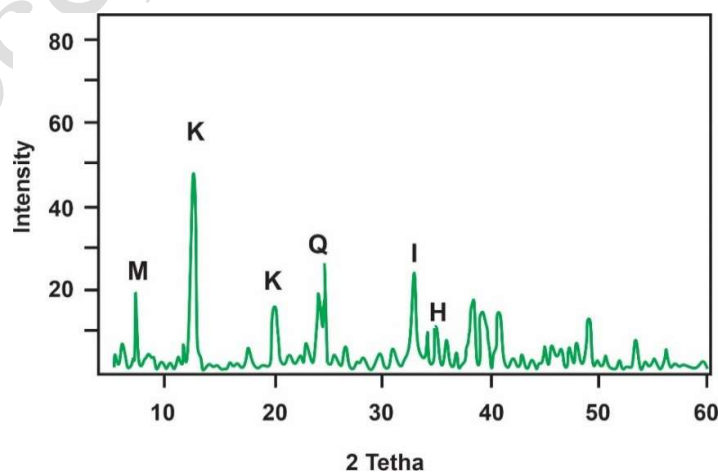


**Figure 5.** The XRD results of a shale sample from the Ilam Formation that exhibit highest peak for kaolinite (K). Minor phases present include illite (I), montmorillonite (M), quartz (Q) and hematite (H) minerals

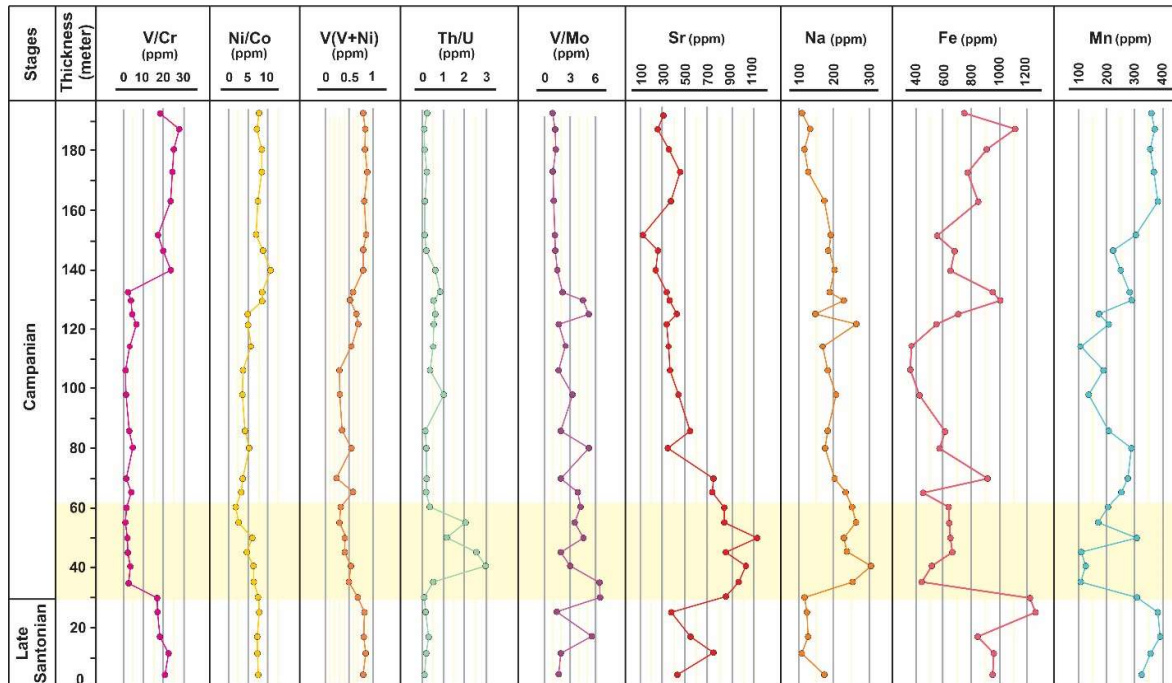


**Figure 6.** The variations of V/Cr, Ni/Co, V(V+Ni), Th/U, V/Mo, Sr, Na, Fe, Mn (ppm) across the Ilam Formation in the Mehdi-Abad section. The yellow box indicates the highest oxygen level area in this section

## Discussion

### *Interactions between foraminiferal biozones, depositional environment, and sea-level changes*

The biostratigraphic analysis, based on planktonic foraminifera in the Mehdi-Abad section, led to the identification of six biozones from the Late Santonian to the Late Campanian (Bohlouli, 2020). The identified biozones include Biozone 1- *Dicarinella asymetrica*, Biozone 2- *Globotruncanita elevate*, Biozone 3- *Globotruncana ventricosa*, Biozone 4- *Radotruncana calcarata*, Biozone 5- *Globotruncanella havanesis*, and Biozone 6- *Globotruncana aegyptiaca* (Figure 7). The record and the relative abundance of planktonic foraminifera assemblages are utilized to reconstruct the paleobathymetric evolution of the Ilam Formation. The paleobathymetric studies display an upper bathyal setting for planktonic foraminiferal assemblages (Biozone 1) in the Late Santonian. During the Campanian, a deepening trend is observed from neritic to upper bathyal environments in the distribution of planktonic foraminifera. Specifically, Biozone 2 is classified as outer neritic, Biozone 3 as middle neritic, Biozone 4 and 5 as outer neritic environments and Biozone 6 as upper bathyal.

According to identified microfacies, the deposition of Ilam Formation occurred in the outer ramp parts of a homoclinal ramp. The identified microfacies of the Ilam Formation in the Mehdi-Abad section contains moderate to high percentage of micrite with planktonic foraminifera that are attributed to deep marine intervals under low-energy hydrodynamic regimes and below the storm wave base (SWB). The occurrence of pyrite and organic matter within samples elucidates low-oxygen conditions (Berner and Raiswell, 1983). The presence of small and fragmented bioclast grains points to unfavorable conditions for the life of biota. Overall, this evidence confirms a deep marine setting for the development of the Ilam Formation during the Late Cretaceous time. Finally, based on recorded evidence, the increase of depth for microfacies is in the order of MF4, MF3, MF2, and MF1.

In the current study, paleo-water-depth fluctuations for the interpretation of sequence

stratigraphic analysis were analyzed using integration of vertical facies distribution and paleobathymetric studies. This led to the identification of two third-order depositional sequences (DS) in the Ilam Formation. The first DS consists of both transgressive system tracts (TST) and regressive system tracts (RST) with the age of the Late Santonian-Early Campanian, and the second depositional sequence only consists of transgressive system tract (TST) that form during the Late Campanian time (Figure 7).

Initially, it is observed that the Ilam Formation deposited unconformably over the Surgah Formation. The occurrence of hematite nodules in the lower parts of the Ilam Formation is related to this unconformable surface. During the Late Santonian stage, a deepening trend is observed in facies associations. MF4 and MF3 are dominant in the lower intervals of the Late Santonian, while MF2 and MF1 show more development in the upper parts. The Late Santonian intervals in the Ilam Formation in this outcrop are considered a TST, with a thickness of 30 meters. The maximum flooding surface (MFS) is characterized by the predominance of MF1, the lowest energy level, an increase in argillaceous limestone layers, and black shale layers.

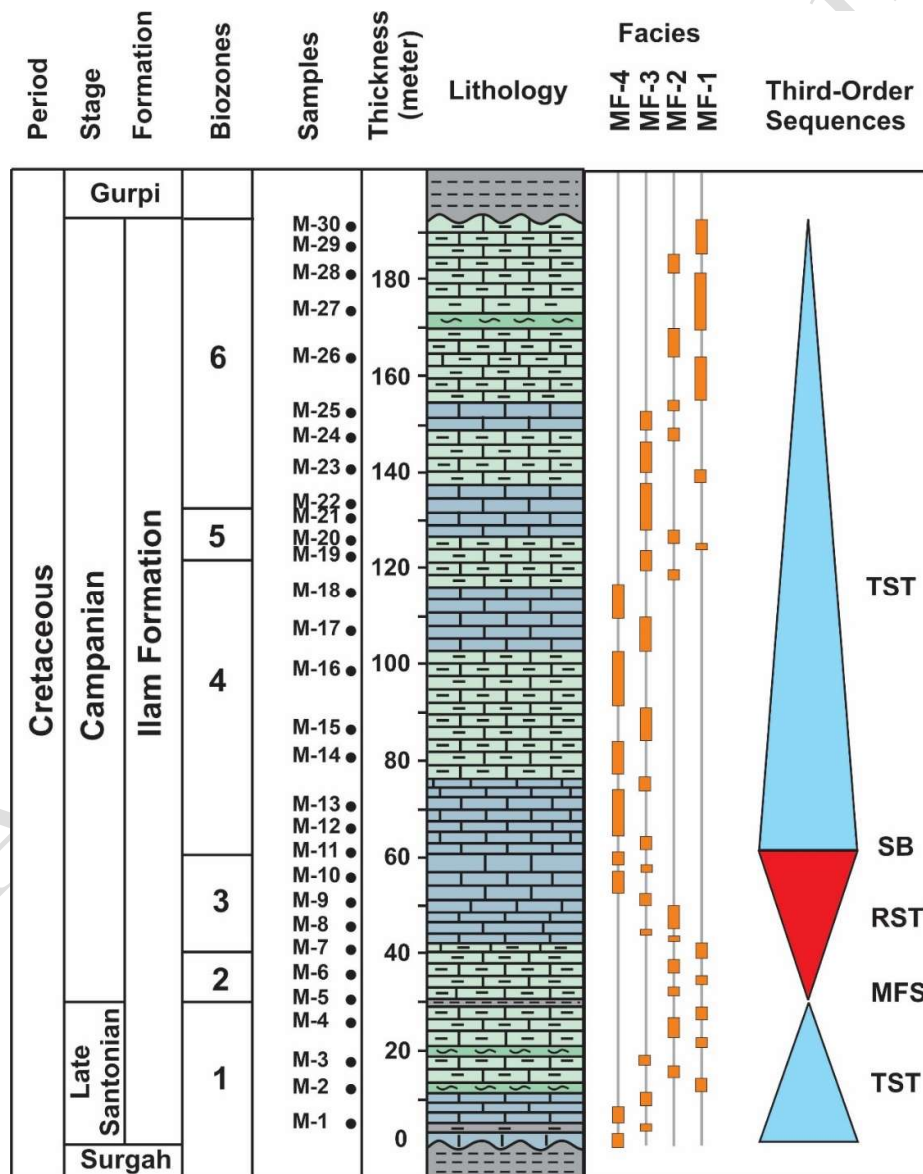


**Figure 7.** The distribution of microfacies across the Ilam Formation and sequence stratigraphy analysis from the Late Santonian to the Late Campanian

Interestingly, the TST is compatible with Biozone 1 that shows an upper bathyal depth for planktonic foraminifera. The beginning of the Campanian stage in the Ilam Formation displays a shallowing trend in facies from MF1 to MF4. This trend continues up to 61 meters of section and is compatible with the occurrence of Biozones 2 and 3 that are formed in the outer neritic and middle neritic environment settings, respectively. This part is attributed to an RST with a thickness of 31 meters that show the end of sequence boundary. The sequence boundary is characterized by a decrease in black shales at the outcrop and increasing MF4 in the petrographic studies. The highest energy level at the outcrop corresponds to this system tract. Here, the sequence boundary is interpreted as type-2, as it is located approximately 60 meters from the base of section and there is no objective evidence of erosional truncation or subaerial exposure. The thickness of carbonate layers increased near the sequence boundary, while the deposition of shaly and argillaceous sediments ceased.

Continuing, the transgressive system tract again dominates and deposition in bathyal settings resumes. MF2 and MF1 increase towards the top of the Ilam Formation. This TST has the most thickness (131 meters) among the identified system tracts in the Ilam Formation. This system tract corresponds to Biozones 4 and 5, indicating outer neritic to upper bathyal settings. The increase in thin-bedded argillaceous limestone at the upper parts of the Ilam Formation confirms the sea level rise towards the MFS. Finally, the Ilam Formation has been separated by a type-1 sequence boundary from the Gurpi Formation.

#### *Trace element characteristics of the Ilam Formation*

Numerous studies indicate that trace elements (such as Co, Cr, Cu, Mo, Ni, Th, U, V) may serve as indicators of paleoredox conditions (e.g., Van Cappellen and Ingall, 1996; Tribovillard et al., 2006; Yang et al., 2012; Bennett and Canfield, 2020; Zheng et al., 2024). The ratios of V/Cr, Ni/Co, Th/U, and V/Mo are considered effective criteria for examining ancient depositional environments.

In anoxic and anaerobic environments, the V/Cr and Ni/Co ratios exceed 4.25 and 7, respectively. Conversely, ratios below 2 and 5 suggest the presence of oxidizing conditions. Dysaerobic conditions are characterized by V/Cr and Ni/Co ratios ranging from 2-4.25 and 5-7, respectively (Xiumian and Chengshan, 2001). Th/U values greater than 2 indicate oxidant conditions, while values lower than 2 indicate anoxic conditions (Wignall and Twitchett, 1996). V/Mo ratios of less than 2 are indicative of anoxic conditions, whereas ratios exceeding 10 suggest oxic conditions. Ratios between 2 and 10 for V/Mo are attributed to dysaerobic or suboxic conditions in environmental settings (Gallego-Torres et al., 2010). V/(V+Ni) is also a dependable measure for depositional both the environment and ocean stratification of the oceanic water body. Values lower than 0.8 indicate anoxic conditions (Wignall, 1994; Pi et al., 2014).

The ratios presented in the intervals of the Ilam Formation, as depicted in Figure 6, indicate several transitions in environmental conditions from oxic to anoxic states. The distribution patterns of the V/Cr, Ni/Co, V/V+Ni, Th/U, and V/Mo ratios show relatively striking similarities in different parts of the Ilam Formation, corresponding to sea-level changes. As previously mentioned, the Late Santonian was a time of increased sea level and dominance of transgressive system tracts and upper bathyal settings. The average ratios of V/Cr, Ni/Co, V/V+Ni, Th/U, and V/Mo are 20.3, 7.4, 0.83, 0.16, and 2.7 ppm, respectively. All ratios obtained indicate anoxic conditions. However, a few samples display suboxic conditions during the Late Santonian.

At the beginning of the Campanian stage, corresponding to regressive system tracts and movement of the sea level towards outer and middle neritic settings, the mentioned paleo-redox proxies suggest suboxic and somewhat oxic conditions. In these intervals, V/Cr, Ni/Co,

V/V+Ni, and Th/U ratios possess lower concentrations compared to the Late Santonian time, while V/Mo ratios show enrichment. Based on the calculated values, V/Cr, Ni/Co, V/V+Ni, Th/U, and V/Mo display an average concentration of 4.3, 5.3, 0.5, 1.45, and 4.4, respectively, which are attributed to suboxic to oxic environments.

As continue, a gradual increase in sea level led to again development of the transgressive system tract in the upper parts of the Ilam Formation. Based on paleobathymetric studies, the onset of TST in the Campanian is compatible with outer neritic sediments and towards the MFS, anoxic conditions are completely preserved. Considering the results that obtained from these ratios, a suboxic to somewhat oxic conditions were created in the beginning of the sea-level rises. This is supported by average values of 2.6, 4.6, 0.45, 0.4, and 3 ppm for V/Cr, Ni/Co, V/V+Ni, Th/U, and V/Mo, respectively. In the upper 70 meters of the Ilam Formation, V/Cr, Ni/Co, V/V+Ni, and Th/U show higher concentrations with averages of 22.7, 8.1, 0.84, and 0.2 ppm. In contrast, the average V/Mo ratio is 1.3 ppm, indicating anoxic environments.

Concentrations of Na, Sr, Mn, and Fe are also considered as useful paleoenvironmental indicators in this study. In the Ilam Formation, Na and Sr elements are mainly concentrated in the samples belonging to regressive system tract, between 30 to 61 meters. Mn and Fe values display a different trend compared to Na and Sr. Fe and Mn show relative enrichment in both identified transgressive system tracts upwards, but their concentrations are reduced in regressive system tracts. Many researches indicate that increases the values of Fe and Mn and decreases the Na and Sr are the indication of the anoxic and dysaerobic environments where sediments have been deposited (Van Cappellen et al., 1998; Abbas Ali, 2012).

Finally, based on all data presented above, the anoxic to suboxic conditions were present during deposition of the Ilam Formation in the Late Cretaceous time. However, during the Early Campanian, paleoclimate evidence suggests a transition towards oxic conditions.

#### *Paleoclimatic and paleogeographic implications*

The Cretaceous basin evolution is one of the most important events during the tectonic history of the northeast margin of the Arabian Plate, including the Zagros area. In this regard, understanding of sea-level fluctuations in relation to paleogeography and ultimately establish a regional scheme is useful that can provide important clues about the geochemical features of oceans during that period.

In recent decades, many studies worldwide have focused on the opening and closure of the Neo-Tethys Ocean. However, there is disagreement and confusion about its causes and timing that formed. In different studies, the onset of the Neo-Tethys opening is attributed to the Late Devonian to the Late Triassic (Stöcklin, 1977; Berberian and King, 1981; Golonka, 2004; Abasaghi et al., 2023). Moreover, a time range from the Late Cretaceous to the Neogen is considered for the closure of the Neo-Tethys Ocean (Gealey, 1988; Alavi, 1994; Golonka, 2004; Agard et al., 2005; Liu et al., 2017; Zhu et al., 2022). Furthermore, the Zagros area was affected by this significant tectonic event during the Cretaceous. On the basis of the paleogeographic studies, the Zagros area was located near tropical latitudes during the Late Cretaceous time (10°-15° N) (Figure 8a), and as a result, was affected by warm and humid climatic conditions (Heydari, 2008).

During this time, increase in volcanic activities in large magmatic provinces was associated with the development of oceanic crust and massive emissions of greenhouse gas concentrations such as CO<sub>2</sub> and methane into the atmosphere (Larson, 1991; Gradstein et al., 2012; Martínez-Rodríguez et al., 2021). The amount of atmospheric CO<sub>2</sub> was almost nine times of its current amount, which was about 3500 ppm (Bice et al., 2006). Besides, because of higher concentration of CO<sub>2</sub>, the oceans are becoming more acidic and ice shelves were shrinking (Wang et al., 2014). The tectonic movements also led to changes in wind systems and

subsequent surface and deep oceanic circulation patterns (Hay, 2011). The increase in temperature and the development of oceanic crust contributed to the rise in sea levels.

The combination of factors mentioned above created significant changes in the chemistry of ocean water during the Cretaceous time. One of the most important changes appeared in the occurrence of OAEs, particularly in the western Neo-Tethys Ocean and the North Atlantic Ocean (e.g., Friedrich et al., 2008; Wapreuch, 2012; Martínez-Rodríguez et al., 2025). OAEs in the Cretaceous are characterized by increasing of organic matter-rich sediments, the dominance of anoxic conditions, perturbations in the carbon cycle, and high ocean temperature. The last OAE in the Cretaceous happened at the Coniacian-Santonian boundary, which is called OAE3 subevent (Arthur et al., 1990). However, many studies indicate that the temporal and spatial distribution of OAE3 and the driving mechanisms are varied in different regions and remain a topic of ongoing debate (Bomou et al., 2011; Jones et al., 2018; Mansour and Wapreuch, 2022, Sun et al., 2025).

Considering the deposition of the Ilam Formation during the Late Santonian to Late Campanian and its proximity to the OAE3, the suboxic and anoxic conditions in this formation can be related to this event. In previous studies, several pieces of evidence from OAEs in the Cretaceous intervals of Zagros has been documented for instance in the Early Aptian (Moosavizadeh et al., 2013) and Cenomanian to Campanian (Asadi Mehmandosti et al., 2021). In most studies, OAE3 has not been regarded as representing genuinely anoxic conditions on a regional scale; instead, its formation is typically ascribed to local conditions rather than to global influences (e.g., Wapreuch, 2012; Sache et al., 2014; Mansour and Wapreuch, 2022).

In the current study, frequent interbedded black shale with limestone indicate a long-term accumulation of laminated organic matter. The abundance of kaolinite minerals within the shale samples reflects humid climatic conditions that are in line with tropical latitudes. Moreover, the geochemical signatures provide strong evidence for the dominance of an aragonitic ocean during deposition of the Ilam Formation in the Late Cretaceous (Adabi and Asadi Mehmandosti, 2008). The occurrence of aragonitic minerals serves as further evidence of a warm climate near tropical latitudes, which is in close agreement with global trends. Generally, climate model simulations during the Cretaceous time estimate that the highest temperatures of the world's oceans occurred from the Cenomanian to Santonian stages (Laugié et al., 2020). According to a study by Abasaghi and Omidpour (2023), the dominance of long eccentricity cycles during the deposition of the Ilam Formation was one of the factors that affected the development of a warm climate at that time.

The high content of redox-sensitive elements and ratios (V/Cr, Ni/Co, V/V+Ni, V/Mo, Th/U) in most intervals of the outcrop, along with few benthic foraminifera, and the occurrence of organic matter were an amplified response to low oxygen deficiency during the development of the homoclinal ramp of the Ilam Formation (Figure 8b). It is important to note that other subzones of the Zagros such as the Dezful embayment, were affected by different paleoenvironmental conditions during the deposition of the Ilam Formation. The predominance of shallow carbonate settings (inner and middle ramp facies) in the Ilam Formation and low content of organic matter are attributed to higher levels of oxygen in this area.

As previously stated, the Zagros area was a part of the eastern Tethyan region that was affected by the events of opening and closure of the Neo-Tethys Ocean. Considering the geological age of the study area, inception of Neo-Tethys closure led to considerable changes in sedimentary architecture, basin subsidence patterns, and sedimentary processes during development of the Ilam Formation. The beginning of closure of the Neo-Tethys Ocean led to create a narrow basin with limited access to open waters and also reorganization in patterns of oceanic circulations and reduced water column ventilation.

The closure of the Neo-Tethys Ocean at the beginning of the Upper Cretaceous aligned with

subtle alterations in displacement rates and vectors of the African plate (Müller et al., 2016), which affected on tectonic active and quiescence periods in the Zagros area. On the other hand, the reactivation of a basement lineament in the Zagros area, in response to ophiolite obduction during the Late Cretaceous time, resulted in the formation of clinoform geometries and as well as paleohighs, affected on the sedimentation patterns (Farzipour-Saein et al., 2009). Noted, the convergence rate of the Afro-Arabian and Iranian plates during the closure of the Neo-Tethys Ocean was less in the Lorestan in comparison with other subzones of the Zagros (Jackson and McKenzie, 1988). Furthermore, different subzones of the Zagros experienced various depositional settings that reflect in thickness and facies types at the same time.

These factors changed the depositional environment of the Late Cretaceous from neritic to mostly pelagic settings in the Lorestan subzone. From the Cenomanian onwards, the evolution of the Zagros foreland basin was controlled by the Balarud deep-seated fault zone with an approximately west-east trend and a dip towards the north and northeast. The Balarud fault zone, located between the Dezful Embayment and Lorestan subzones, is part of the Mountain Front Fault that has been active since at least the Coniacian stage (Motiei, 1995). This fault in the south of the Lorestan subzone is a flexure belt that resulted in structural lowering, changes in thickness and facies, and sediment layers dipping in a north and northeast direction (Sepehr and Cosgrove, 2004; Hajjalibeigi et al., 2011).

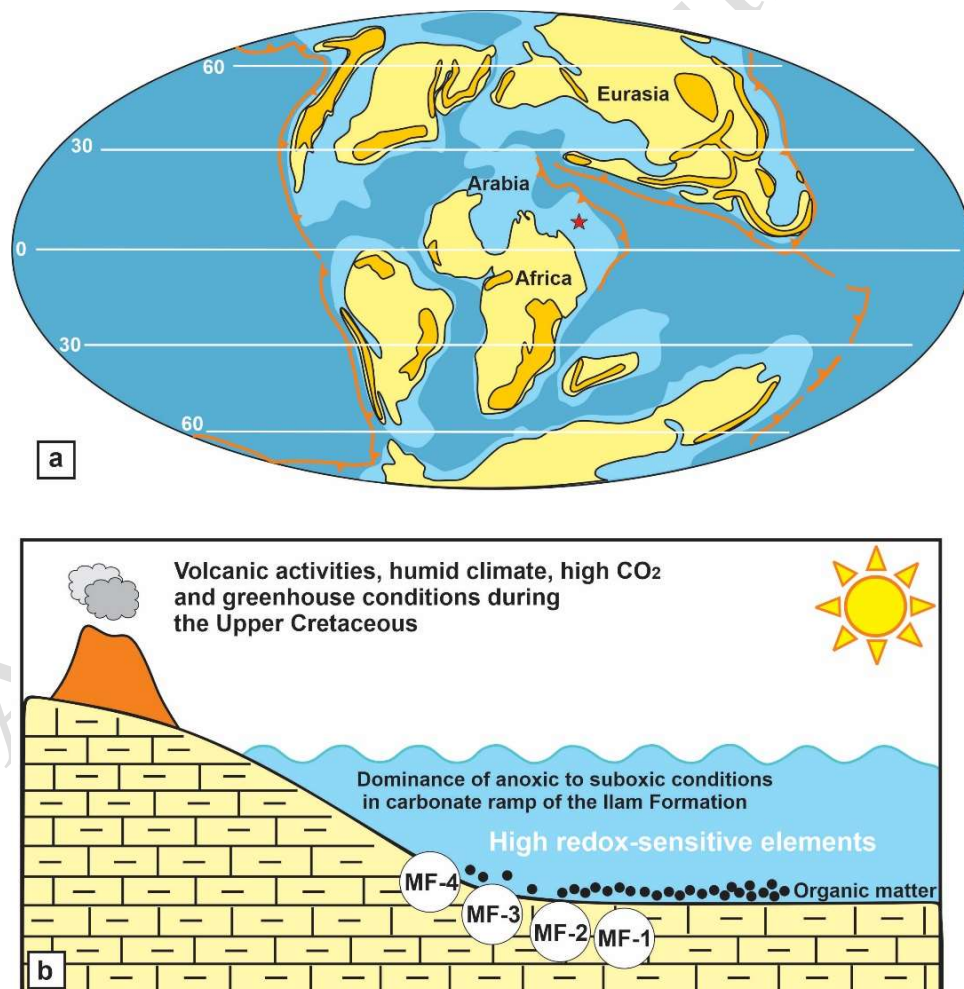


**Figure 8.** a) The paleogeographic positions of the Zagros area (marked with a red star) during the Late Cretaceous (after Scotese, 2014), b) Dominance of anoxic to suboxic conditions in the carbonate ramp of the Ilam Formation

In sum, the role of paleogeographic events and local faults in increase of accommodation space and deepening the basin during the Upper Cretaceous of the Zagros is undeniable. Moreover, the dominance of anoxic conditions is compatible with OAE3 in the Late Cretaceous. However, TOC and carbon isotope data are needed to support our findings. High temperature oceans and changes in circulation patterns can be considered as subfactors affecting water column redox conditions at that time.

## Conclusion

Understanding the driving forces that control the geochemical and sedimentological characteristics of the Ilam Formation is fundamental for reconstructing the paleogeographic conditions of the Zagros area in the Upper Cretaceous. A perusal of the intervals of the Ilam Formation through petrography and geochemical analyses leads to the following conclusions:

The identified microfacies in the Ilam Formation consist of mudstone to mudstone with planktonic foraminifera, wackestone with planktonic foraminifera, wackestone-packstone with planktonic foraminifera and oligosteginids, and wackestone-packstone with planktonic foraminifera and skeletal fragments. These microfacies developed under low energy conditions of the outer parts of the homoclinal ramp.

Analysis of sea-level changes during deposition of the Ilam Formation indicates the development of two third-order sequences, including transgressive and regressive system tracts during the Late Cretaceous. The integration of sequence stratigraphic and paleobathymetric analyses suggests the dominance of neritic and bathyal settings for the sediments of the Ilam Formation.

The values of V/Cr, Ni/Co, V/V+Ni, Th/U, V/Mo, Sr, Na, Mn, and Fe across the Ilam Formation indicate the dominance of anoxic conditions in the Late Santonian as well as the Late Campanian corresponding to transgressive system tracts and movements of sea level towards bathyal and outer neritic environments. In contrast, the mentioned ratios and elements in the intervals of the Early Campanian show an increase in oxygen levels, which is compatible with regressive system tracts and the development of outer and middle neritic settings.

Low oxygen conditions and the development of deep-marine settings in most intervals of the Ilam Formation may have been induced by multiple allogenic and autogenic mechanisms including OAE3, the inception of the closure of the Neo-Tethys Ocean in the Late Cretaceous and the occurrence of local events, such as changes in the basement and activity of faults.

## Acknowledgment

This project was supported by funding from the Ferdowsi University of Mashhad, Iran, under grant no: 3/49327.

## References

- Abasaghi, F., Mahboubi, A., Mahmoudi Gharaei, M.H., Khanehbadc, M., 2023. Palaeogeographic and palaeoclimatic reconstruction of the Permian sediments in the Alborz Basin, Iran: Sedimentological and geochemical approaches. *Journal of African Earth Sciences* 200: 104861.
- Abasaghi, F., Omidpour, A., 2023. Examination of climatic orbital changes and sedimentation rate in the Ilam Formation in the Kupal oilfield, Dezful Embayment. *Iranian Journal of Petroleum Geology* 23: 89-105. (In Persian).
- Abbas Ali, R., 2012. Mn distribution in the carbonate fraction of shallow Marine lithofacies, lower Miocene, Wadi Fuhaimi and Anah twon (western Iraq). *Diyala Journal for Pure Science* 8: 131-150.
- Adabi, M.H., Asadi Mehmandosti, E., 2008. Microfacies and Geochemistry of the Ilam Formation in the Tang-E Rashid Area, Izeh, SW Iran. *Journal of Asian Earth Sciences* 33: 267-277.

- Agard, P., Omrani, J., Jolivet, L., Whitechurch, H., Vrielynck, B., Spakman, W., Monié, P., Meyer, B., Wortel, R., 2011. Zagros orogeny: A subduction-dominated process. *Geological Magazine* 148: 692-725.
- Alavi, M., 1994. Tectonics of the Zagros orogenic belt of Iran: new data and interpretations. *Tectonophysics* 229: 211-238.
- Alsharhan, A.S., Nairn, A.E.M., 1997. *Sedimentary Basins and Petroleum Geology of the Middle East*. Elsevier, Amsterdam.
- Arthur, M.A., Jenkyns, H.C., Brumsack, H.J., Schlanger, S.O., 1990. Stratigraphy, geochemistry, and paleoceanography of organic carbon-rich cretaceous sequences. In: Ginsburg, R.N., Beaudoin, B. (Eds.). *Cretaceous Resources, Events and Rhythms: Background and Plans for Research*. NATO ASI Series 304: 75-119.
- Asadi Mehmandosti, E., Asadi, A., Daneshian, J., Woods, A.D., Loyd, S.J., 2021. Evidence of Mid-Cretaceous carbon cycle perturbations and OAE2 recorded in Cenomanian to middle Campanian carbonates of the Zagros fold-thrust belt basin, Iran. *Journal of Asian Earth Sciences* 218: 104863.
- Beckmann, B., Wagner, T., Hofmann, P., 2005. Linking Coniacian-Santonian (OAE3) black-shale deposition to African climate variability: a reference section from the eastern tropical Atlantic at orbital time scales (ODP site 959, off Ivory Coast and Ghana). In: Harris N.B., *The Deposition of Organic-Carbon-Rich Sediments: Models, Mechanisms, and Consequences*. *SEPM Spec* 82: 125-143.
- Bennett, W.W., Canfield, D.E., 2020. Redox-sensitive trace metals as paleoredox proxies: A review and analysis of data from modern sediments. *Earth-Science Reviews* 204: 103175.
- Berberian, M., King, G.C.P., 1981. Towards a paleogeography and tectonic evolution of Iran. *Canadian Journal of Earth Sciences* 18: 210-265.
- Berner, R.A., Raiswell, R., 1983. Burial of organic carbon and pyrite sulfur in sediments over Phanerozoic time: a new theory. *Geochimica Cosmochimica Acta* 47: 855-862.
- Bice, K.L., Birgel, D., Meyers, P.A., Dahl, K.A., Hinrichs, K.U., Norris, R.D., 2006. A multiple proxy and model study of Cretaceous upper ocean temperatures and atmospheric CO<sub>2</sub> concentrations. *Paleoceanography* 21:10-29.
- Bohlouli, E., 2020. Microbiostratigraphy and paleoecology of the Ilam Formation based on planktonic foraminifera at Kuhe- Sourgah section, Zagros sedimentary basin. MSc, Faculty of Science, Ferdowsi University of Mashhad, 152 pp.
- Bomou, B., Adatte, T., Spangenberg, J., Keller, G., Föllmi, K., 2011. Expression of the Coniacian-Santonian Oceanic Anoxic Event (OAE3) in two potential GSSP sections: Olazagutia, (Spain) and Ten Mile Creek - Arbor Park, (USA). Conference EGU, Vienna, Austria.
- Catuneanu, O., Galloway, W.E., Kendall, C.G.S.C., Miall, A.D., Posamentier, H.W., Strasser, A., Tucker, M.E., 2011. *Sequence Stratigraphy: Methodology and Nomenclature*. *Newsletters on Stratigraphy* 44: 173-245.
- Dunham, R., 1962. Classification of carbonate rocks according to depositional texture. In: *Classification of Carbonate Rocks*, American Association Petroleum Geology, 121 pp.
- Falcon, N.L., 1974. Southern Iran: Zagros Mountains. Geological Society, London, Special Publications 4: 199-211.
- Flügel, E., 2010. *Microfacies of carbonate rocks: analysis, interpretation and application*. Springer, Berlin; New York.
- Farzipour-Saein, A., Yassaghi, A., Sherkati, S., Koyi, H., 2009. Basin evolution of the Lurestan region in the Zagros fold-and-thrust belt, Iran. *Journal of Petroleum Geology* 32: 5-20.
- Friedrich, O., Norris, R.D., Bornemann, A., Beckmann, B., Palike, H., Worstell, P., Hofmann, P., Wagner, T., 2008. Cyclic changes in Turonian to Coniacian planktic foraminiferal assemblages from the tropical Atlantic Ocean. *Marine Micropaleontology* 68: 299-313.
- Gealey, W.K., 1988. Plate tectonic evolution of the Mediterranean-Middle East region. *Tectonophysics* 155: 285-306.
- Gllego-Torres, D., Martinez-Ruiz, F., De Lange, G.J., Jimenez-Espejo, F.J., Ortega Huertas, M., 2010. Trace elemental derived paleoceanographic and paleoclimatic conditions for Pleistocene Eastern Mediterranean sapropels. *Palaeogeography Palaeoclimatology Palaeoecology* 293: 76-89.
- Golonka, J., 2004. Plate tectonic evolution of the southern margin of Eurasia in the Mesozoic and Cenozoic. *Tectonophysics* 381: 235-273.

- Gradstein, F.M., Ogg, J.G., Schmitz, M.D., Ogg, G.M., 2012. *The Geological Time Scale 2012*: Amsterdam, Elsevier.
- Hajjalibeigi, H., Alavi, S.A., Eftekharneshad, J., Mokhtari, M., Adabi, M.H., 2011. The geometric effects of the Balarud deep seated fault zone on Khushab anticline, SW Iran, an integrated study. *Journal of Sciences, Islamic Republic of Iran, University of Tehran* 22: 33-49.
- Hay, W.W., 2011. Can Humans Force a Return to a “Cretaceous” Climate?. *Sedimentary Geology* 235: 5-26.
- Heydari, E., 2008. Tectonic versus eustatic control on supersequences of the Zagros Mountains of Iran. *Tectonophysics* 451: 56-70.
- Hunt, D., Tucker, M., 1992. Stranded parasequences and the forced regressive wedge systems tract: deposition during base-level fall. *Sedimentary Geology* 81: 1-9.
- Jackson, J., Mckenzie, D.P., 1988. The relationship between plate motions and seismic moment tensors, and the rates of active deformation in the Mediterranean and Middle East. *Geophysical Journal* 93: 45-73.
- Jafarian, A., Husinec, A., Wang, C., Chen, X., Wang, M., Gröcke, D.R., Saboor, A., Li Y., 2024. Intrashelf basin record of redox and productivity changes along the Arabian margin of Neo-Tethys during Oceanic Anoxic Event 1a. *Palaeogeography Palaeoclimatology Palaeoecology* 636: 111975.
- James, G.A., Wynd, J.G., 1965. Stratigraphic Nomenclature of Iranian Oil Consortium, Agreement Area. *American Association of Petroleum Geologists Bulletin* 49: 2182-2245.
- Jones, M.M., Ibarra, D.E., Gao Y., Sageman, B.B., Selby, D., Chamberlain, C.P., Graham, S.A., 2018. Evaluating Late Cretaceous OAEs and the influence of marine incursions on organic carbon burial in an expansive East Asian paleo-lake. *Earth and Planetary Science Letters* 484: 41-52.
- Karimnejad Lalami, H.R., Hajjalibeigi, H., Sherkati, S., Adabi, M.H., 2020. Tectonic evolution of the Zagros foreland basin since Early Cretaceous, SW Iran: Regional tectonic implications from subsidence analysis. *Journal of Asian Earth Sciences* 204: 104550.
- Kordi, M., 2019. Sedimentary basin analysis of the Neo-Tethys and its hydrocarbon systems in the Southern Zagros fold-thrust belt and foreland basin. *Earth-Science Reviews* 191: 1-11.
- Kosari, E., Kadkhodaie, A., Bahroudi, A., Chehrazi, A., Talebian, M., 2017. An integrated approach to study the impact of fractures distribution on the Ilam-Sarvak carbonate reservoirs: A case study from the Strait of Hormuz, the Persian Gulf. *Journal of Petroleum Science and Engineering* 152: 104-115.
- Kouamelan, K.S., Zou, C., Wang, C., Assie, K.R., Peng, C., Mondah, O.R., N'dri, K.A., Brantson, E.T., 2020. Multifractal characterization of the Coniacian-Santonian OAE3 in lacustrine and marine deposits based on spectral gamma ray logs. *Scientific Reports* 10: 14363.
- Larson, R.L., 1991. Latest pulse of Earth: Evidence for a mid-Cretaceous superplume. *Geology* 19: 547-550.
- Laugié, M., Donnadiou, Y., Ladant, J.B., Green, J.A.M., Bopp, L., Raison, F., 2020. Stripping back the modern to reveal the Cenomanian-Turonian climate and temperature gradient underneath. *Climate of the Past* 16: 953 - 971.
- Liu, X., Wen, Z., Wang, Z., Song, C., He, Z., 2018. Structural characteristics and main controlling factors on petroleum accumulation in Zagros Basin, Middle East. *Journal of Natural Gas Geoscience* 3: 273-281.
- Mansour, A., Wagreich, M., 2022. Earth system changes during the cooling greenhouse phase of the Late Cretaceous: Coniacian-Santonian OAE3 subevents and fundamental variations in organic carbon deposition. *Earth-Science Reviews* 229: 104022.
- Martínez-Rodríguez, R., Selby, D., Castro, J.M., de Gea, G.A., Nieto, L.M., Ruiz-Ortiz, P.A., 2021. Tracking magmatism and oceanic change through the early Aptian Anoxic Event (OAE 1a) to the late Aptian: Insights from osmium isotopes from the westernmost Tethys (SE Spain) Cau Core. *Global and Planetary Change* 207: 103652.
- Martínez-Rodríguez, R., Castro, J.M., de Gea, G.A., Nieto, L.M., Ruiz-Ortiz, P.A., Skelton, P.W., 2025. Early Aptian development and OAE 1a-linked demise of a carbonate platform in the Western Tethys: Lower Cretaceous of Sierra Mariola (South Iberian Paleomargin, SE Spain). *Cretaceous Research* 167: 106032.
- McQuarrie, N., 2004. Crustal scale geometry of the Zagros fold-thrust belt, Iran. *Journal of Structural Geology* 26: 519-535.
- Mehrabi, H., Navidtalab, A., Enayati, A., Bagherpour, B., 2022. Age, duration, and geochemical

- signatures of paleo-exposure events in Cenomanian-Santonian sequences (Sarvak and Ilam formations) in SW Iran: Insights from carbon and strontium isotopes' chemo-stratigraphy. *Sedimentary Geology* 434: 106136.
- Moosavizadeh, A.M., Mahboubi, A., Moussavi-Harami, R., Kavooosi, M.A., 2013. Early Aptian oceanic anoxic event (OAE 1a) in Northeastern Arabian Plate setting: an example from Dariyan Formation in Zagros fold-thrust belt, SE Iran. *Arabian Journal of Geosciences* 7: 4745-4756.
- Motieci, H., 1993. *Geology of Iran, the Stratigraphy of Zagros*. Geological Survey of Iran, Tehran, 572 pp (in Persian)
- Motieci, H., 1995. *Petroleum geology of Zagros*. Geological Survey of Iran Publication, 589 pp. (In Persian)
- Müller, R.D., Seton, M., Zahirovic, S., Williams, S.E., Matthews, K.J., Wright, N.M., Shephard, G.E., Maloney, K.T., Barnett-Moore, N., Hosseinpour, M., Bower, D.J., Cannon, J., 2016. Ocean basin evolution and global-scale plate reorganization events since Pangea breakup. *Annual Review of Earth and Planetary Sciences* 44: 107-138.
- Ounegh, A., Hasan-Zadeh, A., Mohammadi Khanaposhtani, M., Kazaemzadeh, Y., 2024. Wellbore stability analysis based on the combination of geomechanical and petrophysical studies. *Results in Engineering* 24: 103016.
- Pi, D.H., Jiang, S.Y., Luo, L., Yang, J.H., Hong-Fei Ling, H.F., 2014. Depositional environments for stratiform witherite deposits in the Lower Cambrian black shale sequence of the Yangtze Platform, southern Qinling region, SW China: Evidence from redox-sensitive trace element geochemistry. *Palaeogeography Palaeoclimatology Palaeoecology* 398: 125-131.
- Pitman, J.K., Steinshouer, D., Lewan, M.D., 2004. Petroleum generation and migration in the Mesopotamian Basin and Zagros Fold Belt of Iraq: Results from a basin-modeling study. *GeoArabia* 9: 41-72.
- Razmjooei, M.J., Thibault, N., Kani, A., Dinarès-Turell, J., Pucéat, E., Chin, S., 2020. Calcareous nannofossil response to Late Cretaceous climate change in the eastern Tethys (Zagros Basin, Iran). *Palaeogeography Palaeoclimatology Palaeoecology* 538: 109418.
- Read, J.F., 1985. Carbonate platform facies models. *American Association of Petroleum Geologists Bulletin* 69: 1-21.
- Rikhtegarzadeh, M., Vaziri, S.H., Aleali, M., Bakhtiar, H.A., Jahani, D., 2017. Microbiostratigraphy, Microfacies and Depositional Environment of the Sarvak and Ilam Formations in the Gachsaran Oilfield, southwest Iran. *Micropaleontology* 63: 413-428.
- Sachse, V.F., Littke, R., Jabour, H., Schumann, T., Kluth, O., 2012. Late Cretaceous (Late Turonian, Coniacian and Santonian) petroleum source rocks as part of an OAE, Tarfaya Basin, Morocco. *Marine and Petroleum Geology* 29: 35-49.
- Sachse, V.F., Heim, S., Jabour, H., Kluth, O., Schumann, T., Aquit, M., Littke, R., 2014. Organic geochemical characterization of Santonian to Early Campanian organic matter-rich marls (Sondage No. 1 cores) as related to OAE3 from the Tarfaya Basin, Morocco. *Marine and Petroleum Geology* 56: 290-304.
- Scotese, C.R., 2014. *Atlas of Late Cretaceous Paleogeographic Maps, PALEOMAP Atlas for ArcGIS, volume 2, The Cretaceous, Maps 16 - 22, Mollweide Projection, PALEOMAP Project, Evanston, IL.*
- Sedaghat, M.A., Shaverdi, T., 1999. 1/100000 geological map of Ilam. Geological Survey of Iran.
- Sepehr, M., Cosgrove, J.W., 2004. Structural framework of the Zagros fold-thrust belt, Iran. *Marine and Petroleum Geology* 21: 829-843.
- Shafiee Ardestani, M., Vahidinia, M., Rahiminejad, A.H., Bohloli, E., 2022. Planktonic foraminiferal biostratigraphy and determination of the Santonian-Campanian boundary in the Zagros sedimentary basin, SW Iran. *Stratigraphy* 19: 51-64.
- Sherkati, S., Letouzey, J., 2004. Variation of structural style and basin evolution in the Central Zagros (Izeh Zone and Dezful Embayment), Iran. *Marine and Petroleum Geology* 21: 535-554.
- Stöcklin, J., 1977. Structural correlation of the Alpine ranges between Iran and central Asia. *Mémoires de la Société Géologique de France* 8: 333-353.
- Sun, M., Archer, C., Scholz, F., Sweere, T., Vance, D., 2025. Trace metal evolution of the Late Cretaceous Ocean. *Chemical Geology* 671: 122477.
- Tejada, M.L.G., Suzuki, K., Kuroda, J., Coccioni, R., Mahoney, J.J., Ohkouchi, N., Sakamoto, T., Tatsumi, Y., 2009. Ontong Java Plateau eruption as a trigger for the early Aptian oceanic anoxic

- event. *Geology* 37: 855-858.
- Tribovillard, N., Algeo, T.J., Lyons, T., Riboulleau, A., 2006. Trace metals as paleoredox and paleoproductivity proxies: an update. *Chemical Geology* 232: 12-32.
- Van Cappellen, P., Ingall, E.D., 1996. Redox stabilization of the atmosphere and oceans by phosphorus-limited marine productivity. *Science* 271: 493-496.
- Wagreich, M., 2012. "OAE 3"- regional Atlantic organic carbon burial during the Coniacian-Santonian. *Climate of the Past* 8: 1447-1455.
- Wang, Y., Huang, C., Sun, B., Quan, C., Wu, J., Lin, Z., 2014. Paleo-CO<sub>2</sub> variation trends and the Cretaceous greenhouse climate. *Earth-Science Reviews* 129: 136-147.
- Wignall, P.B., 1994. *Black Shales*, Clarendon Press, Oxford, 127 pp.
- Wignall, P.B., Twitchett, R.J., 1996. Oceanic anoxia and the end Permian mass extinction. *Science* 272: 1155-1158.
- Xiumian, H., Chengshan, W., 2001. Summarization on the studying methods of the Palaeo-ocean dissolved oxygen. *Advance in Earth Sciences* 16: 65-71 (in Chinese).
- Yang, X., Zhao, Y., Guo, Q., Yang, H., 2012. Geochemistry of the trace elements and rare-earth elements at the boundary between Cambrian Series 2 and Series 3 at Jianshan, South China: Paleoenvironmental and stratigraphic implications. *Geochemistry* 31: 465-475.
- Zheng, C.Y.C., Kerans, C., Buatois, L.A., Mangano, M.G., Ko, L.T., 2024. Sedimentary environment and benthic oxygenation history of the Upper Cretaceous Austin Chalk Group, South Texas: An integrated ichnological, sedimentological and geochemical approach. *Sedimentology* 71: 1149-1192.
- Zhu, R., Zhao, P., Zhao, L., 2022. Tectonic evolution and geodynamics of the Neo-Tethys Ocean. *Science China Earth Sciences* 65: 1-24.

